



Development of Machine Learning Models for Studying the Premixed Turbulent Combustion of Gas-To-Liquids (GTL) Fuel Blends

Abdellatif M. Sadeq¹ · Amin Hedayati Moghaddam² · Ahmad K. Sleiti¹ · Samer F. Ahmed¹

Received: 21 June 2023 / Revised: 13 August 2023 / Accepted: 4 September 2023 / Published online: 15 February 2024
© The Author(s) 2024

Abstract

Studying the spatial and temporal evolution in turbulent flames represents one of the most challenging problems in the combustion community. Based on previous 3D numerical analyses, this study aims to develop data-driven machine learning (ML) models for predicting the flame radius evolution and turbulent flame speeds for diesel, gas-to-liquids (GTL), and their 50/50 blend (by volumetric composition) under different thermodynamic and turbulence operating conditions. Two ML models were developed in this study. Model 1 predicts the variations of the flame radius with time, equivalence ratio, and turbulence intensity, whereas model 2 predicts the variations of the turbulence flame speed with the operating parameters. The k-fold cross-validation technique is used for model training, and the developed neural network-based model is used to investigate the effects of operating parameters on the premixed turbulent flames. In addition, the possible minimum and maximum values of responses at the corresponding operating parameters are found using a genetic algorithm (GA) approach. Model 1 could capture the computational fluid dynamics (CFD) outputs with high precision at different flame radii and time instants with a maximum absolute error percentage of 5.46%. For model 2, the maximum absolute error percentage was 6.58%. Overall, this study demonstrates the applicability and promising performance of the proposed ML models, which will be used in subsequent research to analyze turbulent flames a posteriori.

Keywords Turbulent premixed flame · GTL · Flame radius evolution · Turbulent flame speed · Machine learning model · Artificial intelligence

Introduction

Turbulent flame speed (TFS) identifies the speed at which a flame spreads in a turbulent flow field, such as that in a gas turbine combustor or a reciprocating internal combustion engine [1]. Chemical kinetics and fluid mechanics are combined by the turbulent flame speed in the study of turbulent combustion [2]. When the hot burned product gases and the cold unburned reactant gases interact under the existence of turbulence in a combusting flow, the reaction rate is significantly increased and the flame brush thickness expands by the effect of different eddy sizes [3]. The combination of

fluid mechanics and chemical kinetics offers a problem in modeling turbulent combustion events due to the considerable influence of turbulence on the flame propagation rate [4]. Studying the premixed turbulent combustion for an air–fuel mixture is critical for predicting engine performance and its emission rates. In addition, different physical phenomena such as flame extinction and diffusion, flame ignition mechanisms, flame quenching, and stabilization lie behind the analysis of premixed turbulent flows. Furthermore, the optimum operating conditions for a particular fuel can be assessed depending on these analyses [5–7].

Gas-to-liquids (GTL) fuel is one of the alternative fuels for diesel fuel that has gained much attention recently due to its clean burning nature [8]. Therefore, lowering exhaust emissions to comply with regional and global environmental laws (The Paris Agreement, [9]). Additionally, GTL fuel has no toxicity and is free of unfavorable elements like metals, aromatics, and sulfur, making it less poisonous and less detrimental to the environment. Moreover, it does not smell bad and is safer to handle and store than diesel fuel [10].

✉ Abdellatif M. Sadeq
as1004958@qu.edu.qa

¹ Mechanical and Industrial Engineering Department, College of Engineering, Qatar University, Doha, Qatar

² Department of Chemical Engineering, Faculty of Engineering, Central Tehran Branch, Islamic Azad University, Tehran, Iran

According to Qatar Shell, GTL fuel can reduce nitric oxide (NO_x) emissions by 25% and particulate matter (PM) emissions by roughly 38% compared to diesel fuel [11].

Remarkable progress has been achieved in measuring the turbulent flame speed of different fuels using various experimental techniques [12] and numerical simulation models [13]. One of the main objectives for conducting the experiments is to use their outputs for establishing detailed combustion mechanisms and to use them for validation purposes [14–16]. However, due to the constraints of experimental measurements, a fuel's laminar or turbulent flame speed is often only acquired under a few different combustion operating conditions. To build detailed combustion mechanisms for application in computational fluid dynamics (CFD) simulations, these mechanisms are developed and validated using the measured flame speeds under these selected conditions [17–19].

The high computational cost, however, makes it difficult to anticipate the flame speed utilized in CFD via kinetic modeling utilizing the reduced or detailed mechanisms. Due to the wide range of temperature, pressure, and equivalence ratios used in CFD simulations, the fluctuations of the flame speed are typically explained using empirical relations, which makes it less accurate [17, 18]. The majority of the empirical relations are fitted using experimental values obtained at certain operating conditions or they are fitted from kinetic modeling results that belong to a detailed combustion mechanism [20, 21]. The most widely used combustion mechanism is the power-law expression, in which proper constants are used as inputs for deriving the flame speeds values under particular operating conditions [22, 23]. However, the fitting process used for deriving such expressions usually encounters numerous difficulties [24–26].

Machine learning (ML) techniques have recently gained much attention and have been applied in combustion research due to the rapid advancement of computer and database technology. To predict the overall physical characteristics of fuels [27], the soot emission property [28], and to support CFD simulations [29, 30], ML models have been constructed. For laminar flame speeds (LFSs), a series of researches have been conducted to construct efficient ML models for predicting the values of LFS of fuel under several operating conditions, in which the pressure, temperature, and equivalence ratios are usually adopted as inputs in these models. In regression problems, artificial neural networks (ANN) can discover complex input and output relationships. Therefore, these networks have been used in various fields of science and engineering to model the relationship between input and continuous responses [31–34]. Therefore, this tool can be used to predict the combustion performance of different fuels in terms of operating factors. Several research work in open literature have investigated the capability of ANN to model this process. Malik et al. [35] used a deep neural

network to model laminar burning velocity (LBV) as a fuel property. The investigated fuels were hydrogen–air and propane–air mixture. The operating parameters were pressure, temperature, and equivalence ratio. They concluded that the accuracy of ANN models in predicting LBV values is higher than the analytical formula. Further, they reported that the ANN-based models can predict LBV values of many mixtures.

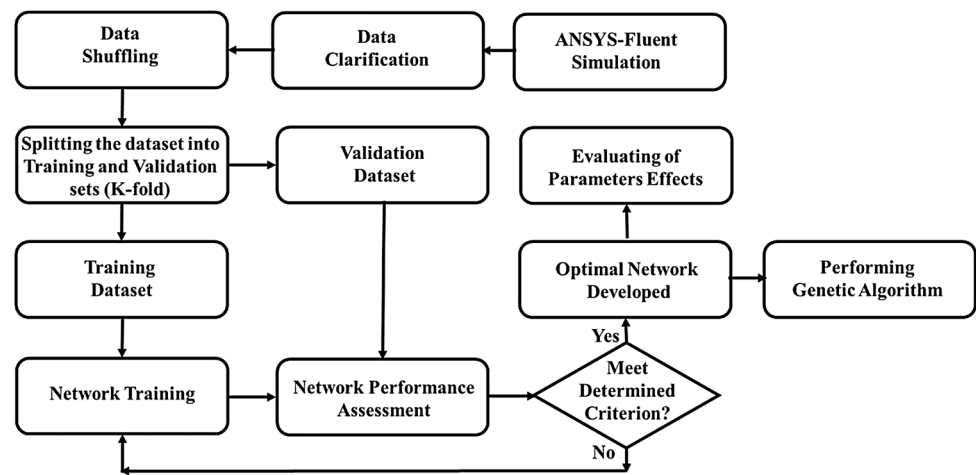
Mehra et al. [36] developed a multilayer feedforward network to predict the combustion process performance of natural gas enriched by H₂ and CO. The operating parameters were fuel–air equivalence ratio and hydrogen, methane, and carbon monoxide fraction. Meanwhile, the response (output parameter) was LBV. They reported that the maximum R^2 for validation was 0.999 implies a good agreement between real and predicted LBV. Eckart et al. [37] used ML methods to predict the LBV of methane/hydrogen/air mixture at different conditions. They developed models based on 1400 data points. To find the optimum structure of the network, they investigated a different number of hidden layers and neurons per layer. Vom Lehn et al. [38] developed a model based on an ANN to predict the LBV of different fuels. They selected molecular group, pressure, temperature, and equivalence ratio as operating parameters and LBV as a response. The dataset was gathered from experimental works and simulations based on kinetic models. Wan et al. [39] investigated different ML techniques to develop a model with the ability to predict the LFS of hydrocarbon and oxygenated fuels. To do this, they proposed Gaussian process regression as an ML methodology.

These previous researches indicate that ML models are delivered as powerful tools for predicting the values of LFS of fuels using the input operating factors. In addition, it can be also noticed that the previous researches have only focused on developing ML models for LFS prediction. However, the derive of general combustion ML models also requires extending these models to predict turbulent flame speeds (TFS), which still shows a research gap.

Based on these considerations, this study focuses on modeling and simulating the effects of operating parameters on flame radius and flame speed during premixed turbulent combustion of diesel, GTL, and their 50/50 blend. Figure 1 shows the implemented method used in the present work. In previous work [13], the turbulent premixed flame of diesel, GTL, and 50% diesel–50% GTL fuel was investigated and simulated using ANSYS-Fluent. In the present study, data from previous work of the authors were used to develop two types of ANN models with the ability to predict flame radius and flame speed.

To do this, the input data are divided into training and validation sets. The k-fold validation technique was used to train the networks. The training method was performed to determine the optimal parameters of the network. After

Fig. 1 Implemented algorithm to develop the optimal model



developing the optimal model parameters, these developed models were used to evaluate the effects of operating parameters on flame radius and flame speed. According to the authors' knowledge, developing neural network models to predict turbulent flame radius and turbulent flame speed has not taken place, yet.

The novelty of this work emanates from the utilization of these ML models. Instead of solely depending on ANSYS simulations, which are grounded in conventional computational techniques, our study exploits ML methodologies to predict intricate combustion behaviors. Model 1 is centered on prognosticating alterations in the flame radius concerning time, equivalence ratio, and turbulence intensity. Conversely, model 2 is devised to anticipate fluctuations in turbulent flame velocity relative to varying operational factors.

The originality resides in the incorporation of ML models, which possess the capability to apprehend intricate associations and structures within the combustion process—often beyond the reach of established simulation methods such as ANSYS. This innovative approach facilitates a more precise and all-encompassing understanding of flame dynamics across a range of thermodynamic and turbulence conditions. Ultimately, this contributes to heightened predictive prowess and insights surpassing the scope of conventional simulations.

Methodology and Procedure

Fan-Stirred Combustion Bomb

In a previous work by the authors [13], a cylindrical fan-stirred combustion bomb was used to study the premixed turbulent combustion of diesel, GTL, and their 50/50 blend. The combustion bomb was modeled using SOLIDWORKS and then imported into ANSYS-Fluent for meshing. The computational domain incorporates the whole vessel's inner

volume approximated by a cylinder (length = 650mm, diameter = 400mm) and four axis-symmetric fans mounted on the internal surface of the bomb. These fans are used to generate the desired turbulence intensity level (u') to study the flame propagation under near homogeneous and isotropic turbulence (HIT). Tetrahedral, equidistant elements were used for meshing the computational domain, with an adaptive size function (element size = 2mm). After successfully meshing the model, the numerical model parameters were identified, and the solution was initialized to match the required thermodynamic and turbulence operating conditions. The complete description of the meshing process and the numerical model settings can be found in previous work [13]. After completing the simulation runs for the three fuels, the dataset is imported from CFD simulation runs and stored in MS Excel sheets for further investigation and analysis.

Numerical Data Source

The numerical data used for ANN model construction, training, and validation were obtained from supporting information from previous work [40]. These datasets represent the premixed turbulent combustion of diesel, GTL, and their 50/50 blend studied at different operating conditions ($0.7 < \phi < 1.3$) and ($0.5 \text{ m/s} < u' < 3.0 \text{ m/s}$) using Zimont Turbulent Flame Speed Closure (Zimont TFC) model available for CFD simulations. Different parameters could be obtained from the simulations runs and tabulated in MS Excel data sheets such as turbulent flame speed (S_f), turbulent kinetic energy (k), turbulent eddy viscosity (μ), and others. These databases allow obtaining each of these parameter values at any vessel's radius, starting from zero to 12cm. In addition, the flame radius at any time starting from zero to 30 ms can be conveniently accessed and obtained. The pre-processed, raw, and filtered data were extracted from CFD simulations [13], then listed on filtered MS Excel tables. The datasets are presented in four tables in the MS Excel file. Tables

S1, S2, and S3 show the values of the parameters related to the premixed turbulent combustion of diesel, GTL, and the 50/50 blend at the corresponding turbulence intensity (u') and equivalence ratio (Φ). In addition, Table S4 shows the flame radius value as a function of turbulence intensity, the equivalence ratio, and time for the three fuels. These datasets are available online with supporting information from previous work [41].

Data Pre-processing

Generally, in data science, all the data need to be pre-processed before beginning the regression, classification, etc. Pre-processing plays a key role in data mining. In Fig. 2 the values of flame radius and turbulent flame speed have been shown. In some cases, the values of some independent and dependent variables may not be available. These data are called null or missed. In this work, there is no null data. In some cases, data may appear that have a large and unusual difference from other values in the dataset. These data can disturb the performance of algorithms termed outliers. So, they should be removed from the dataset. According to Fig. 2, no outlier is detected. Further, the flame radius values corresponding to zero time were removed from the dataset. Because this data leads to incorrect model training performance. Since the order of magnitude of operating parameters is different, so the operating parameters need to be normalized. Note, the values of flame radius and turbulent

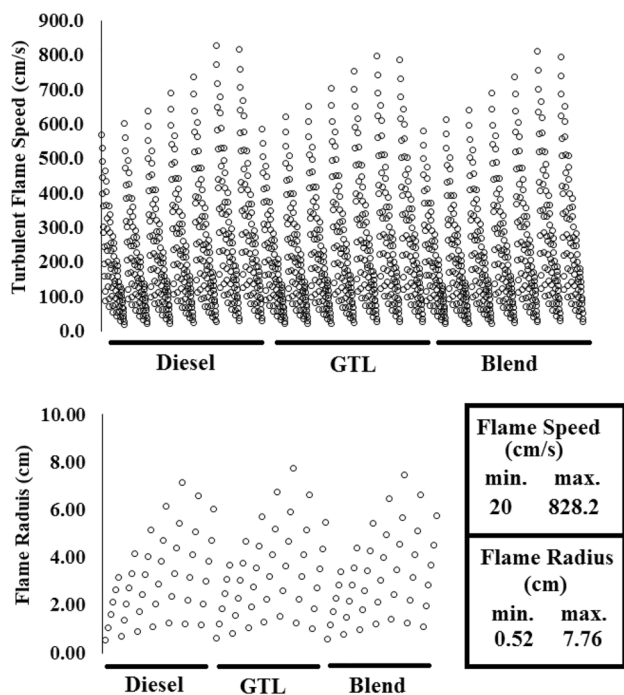


Fig. 2 Data of flame radius and turbulent flame speed

flame speed were not normalized. The normalization process was performed according to the following equation:

$$y_N = 0.05 + \frac{y - y_{\min.}}{y_{\max.} - y_{\min.}} \times 0.9, \quad (1)$$

where $y_{\min.}$ and $y_{\max.}$ are the minimum and maximum values of y .

Model Construction and Training

ANN is a predicting algorithm for regression problems classified as a machine learning methodology. ANN is a human brain-based tool capable of producing output on a given set of inputs. In Fig. 3 the structure of networks used in this work to develop robust models has been shown, where w and b are the devoted weight and bias, respectively. The first layer of the network structure is the input layer. The input layer is fed from the input data (operating parameters). The next box is the hidden layer (one or more). If the number of hidden layers is more than one, the network is termed a deep neural network. The duty of hidden layer(s) is data processing. This (these) layer(s) is (are) connected to the output layer, and the output layer generates the outputs (responses). Fitnet is a specialized version of a feedforward network, noting that the units of each box are unrelated to each other. For fitnet and feedforwardnet, each processing box is connected only to the previous and next layers. However, for cascadeforwardnet, the input layer is connected to the output layer. It is clear that cascadeforwardnet is a modified feedforward network. In these networks, tansig and purelin functions are used for the hidden and output layers, respectively. The next step after constructing the desired network structure is network training using a training dataset. Levenberg–Marquardt (LM) was chosen as training algorithm. During the training of the network, mean squared error (MSE) is used as an assessment index. MSE is calculated as follows:

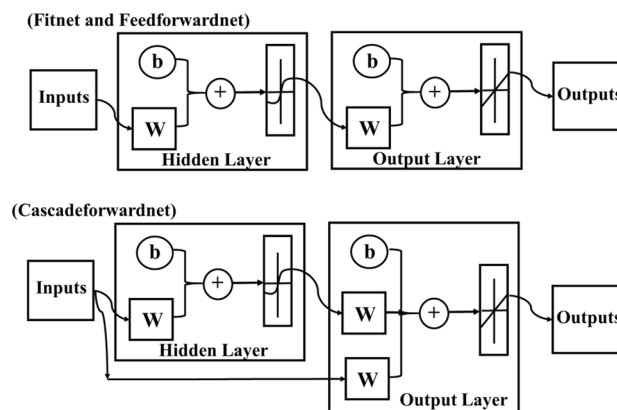


Fig. 3 Structure of feedforward and cascadeforward networks

$$MSE = \frac{1}{n} \sum_{i=1}^n (y_{pred.} - y_{act.})^2, \tag{2}$$

where $y_{pred.}$, $y_{act.}$, and n are the predicted value, actual value, and the number of targets, respectively.

Then, the trained network should be validated using the validation dataset. To compare the performance of different developed models, validation- R^2 is used. This index is determined as follows:

$$R^2 = 1 - \frac{\sum_{i=1}^n (y_{pred.} - y_{act.})^2}{\sum_{i=1}^n (y_{pred.} - y_m)^2}, \tag{3}$$

where y_m is the mean value of targets.

The average relative error (ARE) is calculated as follows:

$$ARE = \left| \frac{y_{pred.} - y_{act.}}{y_{act.}} \right| \times 100. \tag{4}$$

Before starting model training, the data should be randomized. To train the network, the cross-validation method was used. The cross-validation technique is useful for overcoming overfitting which is a common problem in model development. Figure 4 shows the k-fold cross-validation schematically. In this technique, the data is split into two parts (training and validation datasets). The training dataset is used for network training. If the model performs well on the validation dataset, it means that overfitting does not happen. Cross-validation is performed in several ways such as leave-one-out, hold-out, k-fold, and stratified k-fold. In this work, the k-fold cross-validation technique was used to train the model. In this technique, the whole data is divided into k partitions with equal sizes. The first partition is selected as the validation dataset and the other (k-1) datasets are selected as training datasets.

The model capability in predicting the targets of the validation partition is recorded. In the next step, the second partition is set as validation and the other (k-1) partitions are set as training. This procedure is repeated for all the k partitions. It is clear that by increasing the number of partitions, the model variance decreases. The drawback of this method is the k times repeating of the procedure.

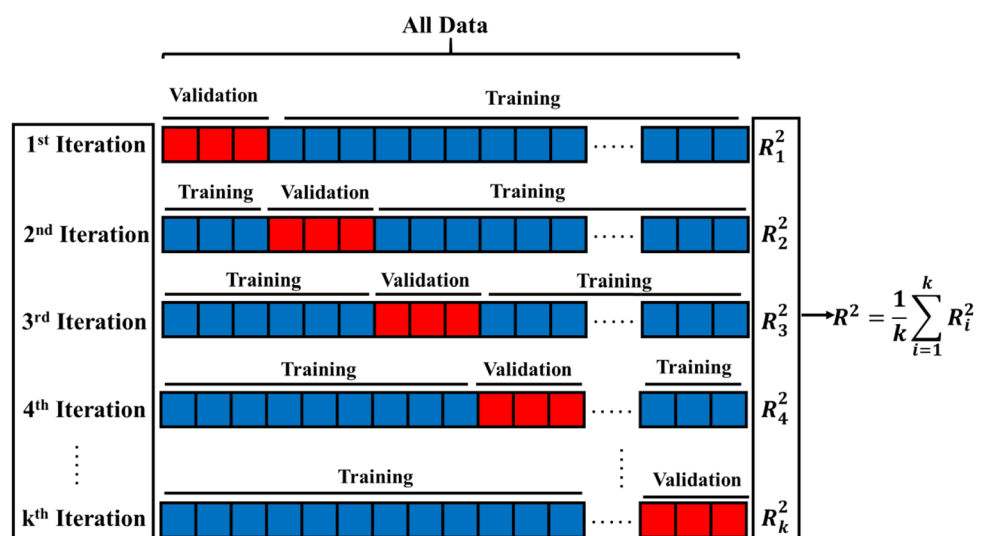
Results and Discussion

In previous work [13], turbulent flame speeds and flame radius for the three fuels (diesel, GTL, and 50/50 blend) at a wide range of operating parameters (turbulence intensities, equivalence ratio, vessel radius, and time) were studied and characterized. In the present work, the flame radius is modeled as a function of equivalence ratio and time. Further, three models are developed for the prediction of turbulent flame speed for different fuels. These models predict turbulent flame speed vs. equivalence ratio, turbulence intensity, and vessel radius. The broad ranges of the operational variables for different responses are presented in Table 1.

Table 1 The operating range of input variables for different responses

Response	Operating parameter	Range
Flame radius evolution-Model 1	Equivalence Ratio	0.7–1.3
	Time (ms)	5–30
Turbulent flame speed-Model 2	Equivalence Ratio	0.7–1.3
	Turbulent Intensity (m/s)	0.5–3
	Vessel Radius (cm)	0–12

Fig. 4 K-fold cross-validation diagram



Flame Radius Evolution-Model 1

As mentioned earlier, the turbulent flame radius was modeled as a function of equivalence ratio and time.

Model Development To develop the neural network model, several functions were tested, and finally, casca-deforwardnet was chosen to proceed. To assess the performance of the developed model, the R^2 -value of the validation dataset was chosen to be monitored. The results show that for diesel, GTL, and the 50/50 blend fuels the optimum number of neurons in the hidden layer are 4, 5, and 5, respectively. To check and make confidence in the network performance, each network was trained 10 times. The average R^2 -value of these optimum models are 0.9856, 0.9809, and 0.9784, respectively. The validation- R^2 values of different runs for networks with one hidden layer and specified neurons in this layer for diesel, GTL, and blended fuel are presented in Fig. 5. Note that each run means a network training process.

Then, networks with optimum structures were trained over the whole dataset, and for subsequent calculations and graph plotting, these models were used. In Fig. 6, the flame radius predicted by the optimum artificial network is plotted against the flame radius generated by ANSYS-Fluent for diesel, GTL, and their 50/50 blend. This figure reveals a good agreement between predicted and real values and proves the acceptable predictability of these models in this case.

Diesel Fuel The predicted flame radius evolution in terms of equivalence ratio and time is shown in Figs. 7 and 8 for three different fuels. The trend of changes in the flame radius versus operating parameters is almost similar for each of the three fuels. For diesel fuel, for equivalence ratios less than 1.15 with an increase in time, the flame radius increases. Obviously, at short times, increasing the equivalence ratio leads to a slight increase in the flame radius. Generally, an increasing trend is observed

for equivalence ratios of 0.7–1.15 and an opposite trend is observed for 1.15–1.25. After that for higher values of equivalence ratio, no considerable change in flame radius is observed.

GTL Fuel As shown in Figs. 7b, 8b, for GTL fuel, the flame radius increases at any equivalence ratio as time increases. Similar to diesel fuel for an equivalence ratio of 0.7–1.1, any increase in the equivalence ratio leads to an increase in the flame radius. For higher values, a decrease is observed. Note, for short-duration values, a sinusoidal change in the flame radius is observed as the equivalence ratio increases.

50%Diesel–50%GTL Fuel Similar to diesel and GTL, for blended fuel, the flame radius increases as time increases. The changes in the flame radius of the blend vs. equivalence ratio are similar to diesel fuel. But, its amount is a little more.

It can be observed from Fig. 8 that the designed AI model could capture the CFD simulations output with high precision at different flame radiuses and time instants. The maximum absolute error percentage was found to be 5.46%, 4.98%, and 3.46% for diesel, GTL, and the 50/50 blend, respectively.

Turbulent Flame Speed-Model 2

Model Development To develop a model for predicting the values of flame speed, a casca-deforwardnet with one hidden layer and three neurons in this layer for each fuel has been structured, trained, and validated. The operating range of input parameters have been shown in Table 1. The values of error (predicted value-real value) are shown in Fig. 9.

GTL Fuel In Fig. 10, different plots of the predicted turbulent flame speed for GTL fuel are drawn in terms of equivalence ratio and turbulence intensity. These graphs were plotted while the vessel radius was fixed at 6 cm. As shown in Fig. 10, any increase in turbulent intensity results

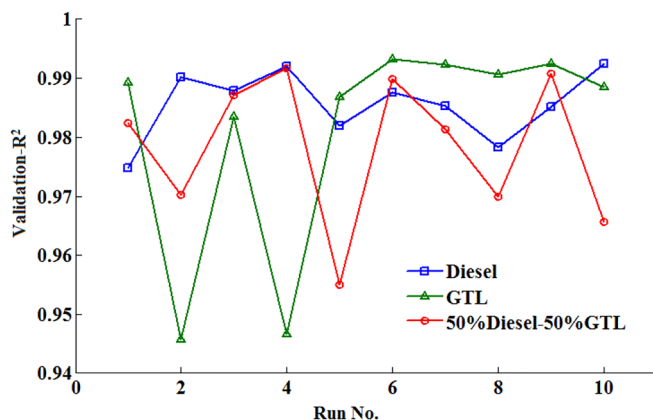


Fig. 5 R^2 -validation values vs. run number for flame radius

	Neurons	Validation- R^2	
		Min.	Max.
Diesel	4	0.9748	0.9925
GTL	5	0.9457	0.9932
50%Diesel-50%GTL	5	0.9550	0.9917

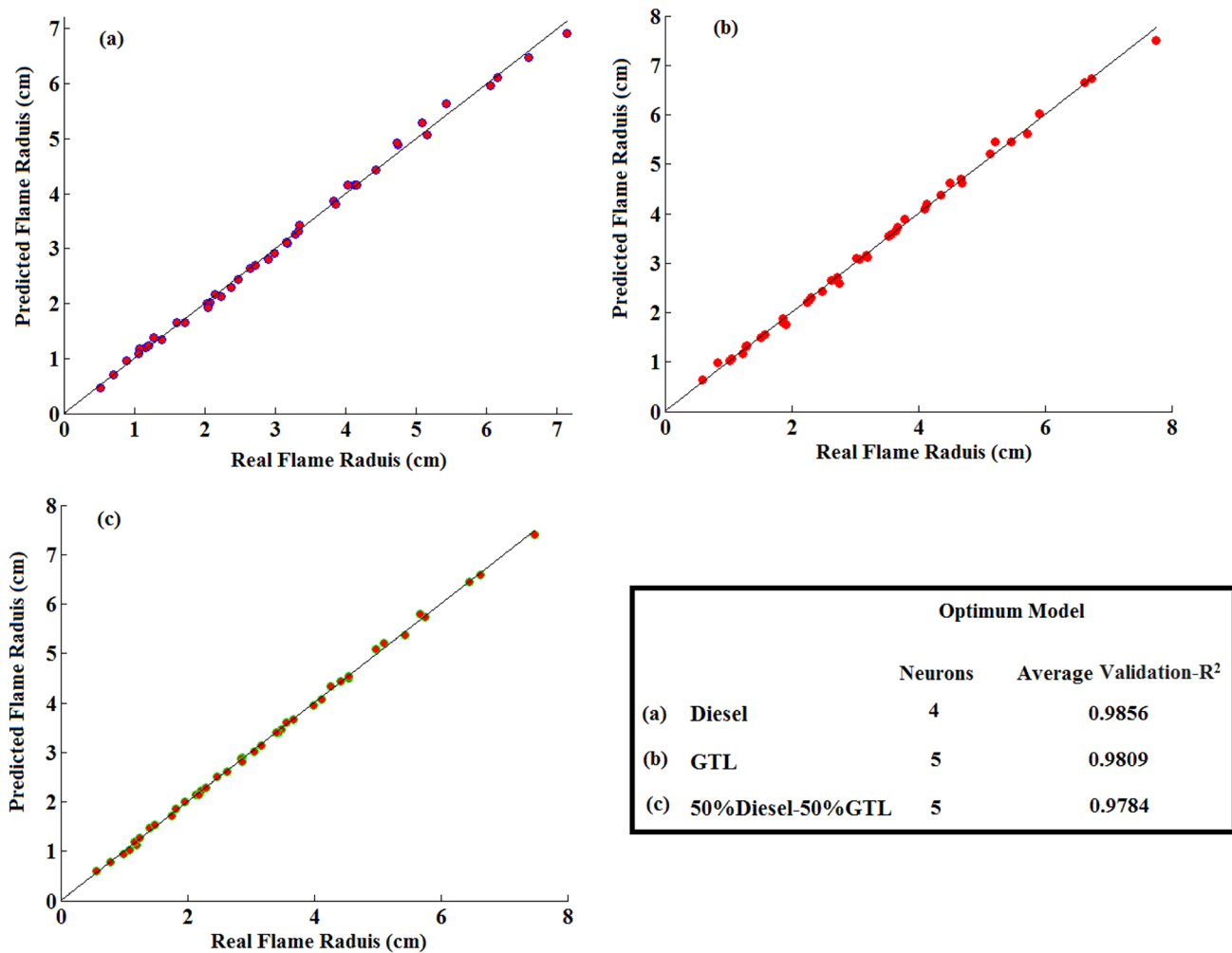


Fig. 6 Predicted flame radius vs. real flame radius for three different fuels

in increasing the flame speed. It can be seen that as the equivalence ratio increases, the flame speed increases and reaches a maximum value. For low values of turbulent intensity, flame speed decreases slightly after reaching the peak. The maximum and minimum flame speeds at a vessel radius of 6 cm are 450.7019 and 74.0430 cm/s, respectively. The designed AI model could capture the CFD simulations output with high precision at different turbulent flame speeds. The maximum absolute error percentage was found to be 6.58% at $u' = 1.5$ m/s.

In Fig. 11, 2D, 3D, and contour plots of the predicted turbulent flame speed for GTL fuel are drawn as a function of equivalence ratio and vessel radius. These plots were generated while the turbulent intensity was fixed at 2 m/s. It is clear that for almost any value of the vessel radius, an increase in the equivalence ratio leads to an increase in the value of the flame speed. After the flame speed reaches the maximum value, a slight decrease is observed in flame speed. But at high values of vessel radius, any increase in

equivalence ratio leads to an increase in flame speed. At this value of turbulent intensity, the possible maximum and minimum values of flame speed are 518.6149 and 56.1675 cm/s, respectively. In addition, it can be observed from Fig. 11 that there is a good agreement between the AI model the CFD simulations output where the maximum absolute error percentage was found to be 5.85% at a vessel radius of 6 cm.

Diesel Fuel As shown in Fig. 12, by increasing the vessel radius, the flame speed increases for each value of turbulent intensity. Similarly, any increase in turbulent intensity leads to a gradual increase in flame speed. This phenomenon happens for each value of vessel radius. The rate of flame speed changes versus turbulent intensity is more severe for high values of vessel radius. For an equivalence ratio of 1.0, the possible maximum and minimum values of flame speed are 702.2660 and 17.7999 cm/s, respectively. The AI model could be well trained to capture the output of CFD simulations, and the maximum absolute error percentage was found to be 6.53% at a vessel radius of 12 cm.

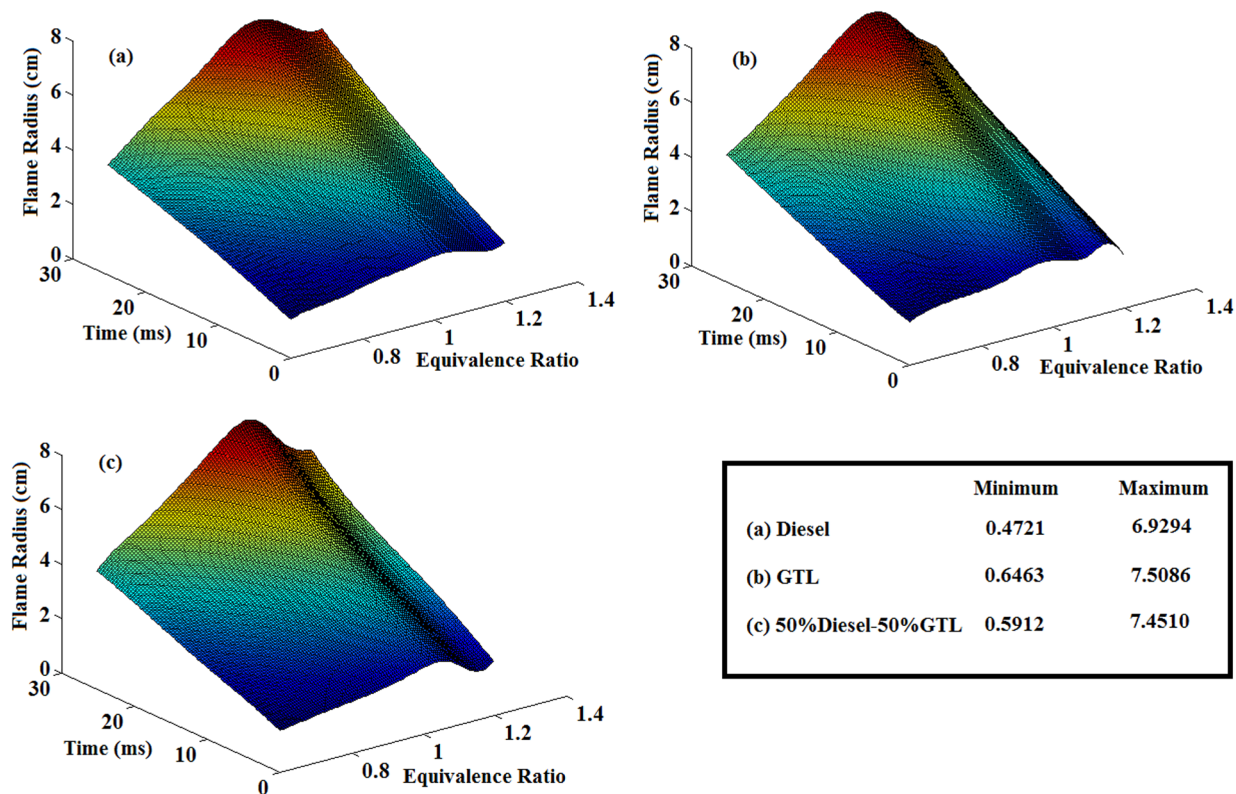


Fig. 7 3D plot of the predicted flame radius as a function of equivalence ratio and time for three different fuels

50%Diesel–50%GTL Fuel Fig. 13 shows the change of predicted turbulent flame speed as a function of turbulent intensity and vessel radius. These plots were generated while the equivalence ratio was fixed at 1.0. At this condition, the possible maximum and minimum flame speeds are 699.8423 and 22.6128 cm/s, respectively. It is found that by increasing the vessel radius, the flame speed decreases. The slope of this decrease is more severe for high values of turbulence intensity. Adversely, any increase in turbulent intensity leads to an increase in flame speed. This phenomenon is more severe at low values of vessel radius. In addition, it can be observed that there is a good agreement between the readings of the designed AI model and CFD simulations output, where the maximum absolute error percentage was depicted at $u' = 2.5$ m/s with a value of 2.57%.

Flame Radius and Turbulent Flame Speed Changes

In Table 2, the conditions that minimum and maximum values of responses happen are shown. To find the max–min response values and corresponding operating parameters GA was used based on the optimum developed ANN models.

Conclusions

The optimum operating conditions for a particular fuel can be assessed by studying its premixed turbulent combustion under the effect of different input parameters. The conventional experimental methods followed to derive TFS for several fuels are very burdensome, whereas detailed kinetic models used for the premixed turbulent combustion applications are usually computationally expensive and inefficient. Fortunately, the large dataset obtained for TFS from CFD simulations can be used to develop efficient data-driven ML models for predicting TFS more accurately. Based on that, model development based on artificial intelligence (AI) was carried out to predict the flame radius evolution and turbulent flame speed during the premixed turbulent combustion of diesel, GTL, and their 50/50 blend under different operating conditions. The numeric data utilized for the development, training, and validation of the ANN models was extracted from supplementary materials. These datasets encompass instances of premixed turbulent combustion concerning diesel, GTL, and their 50/50 mixture. These instances were studied across diverse operational conditions, featuring equivalence ratios spanning from 0.7 to 1.3 and turbulence intensities ranging between 0.5 m/s and 3.0 m/s. The methodology employed the Zimont TFC model.

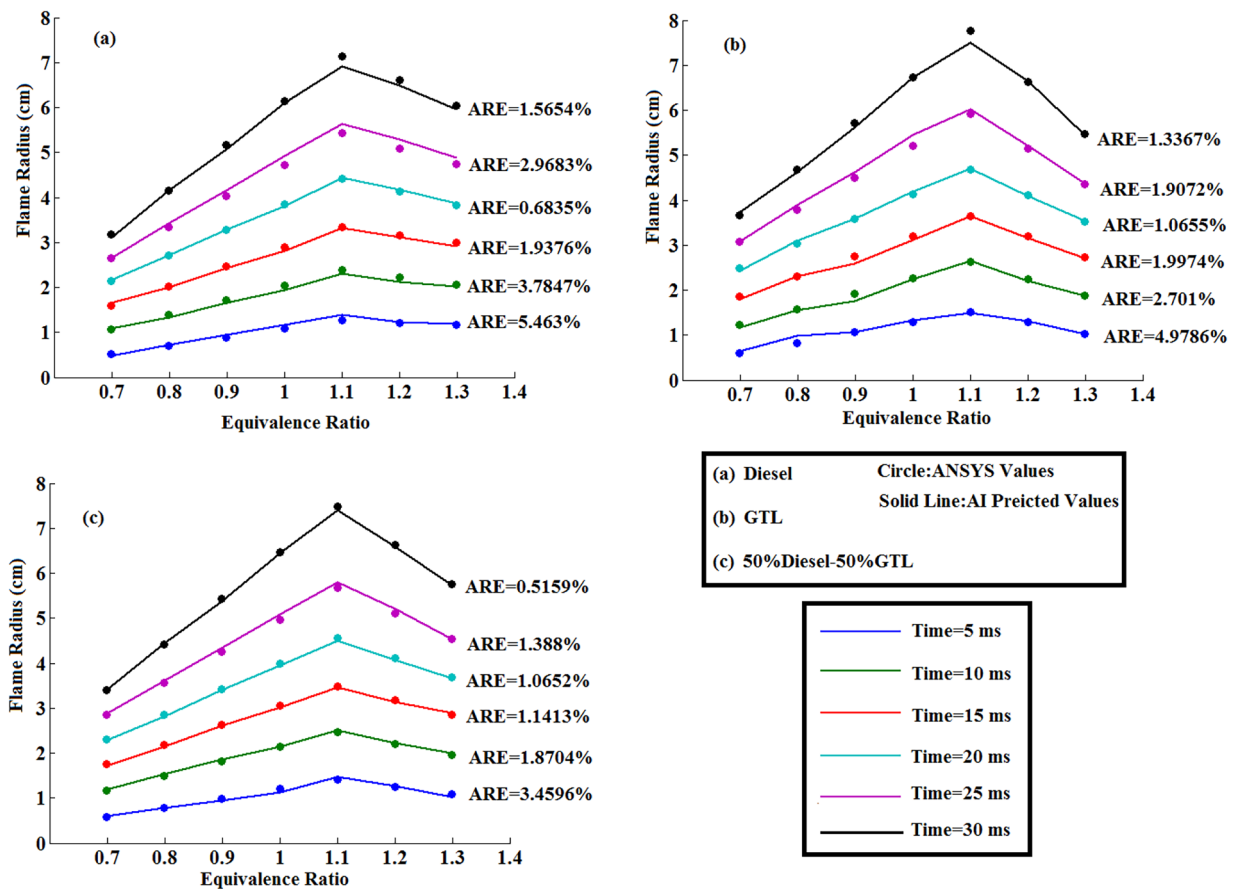


Fig. 8 CFD and AI-predicted flame radius as a function of equivalence ratio at different time

In brief, the core findings of this exploration can be succinctly outlined:

- Two ML models were developed in this study. Model 1 predicts the variations of the turbulent flame radius with respect to the equivalence ratio and time, whereas model 2 predicts the turbulent flame speed variations with respect to the equivalence ratio, turbulence intensity, and vessel radius.
- Model 1 could capture the CFD outputs with high precision at different flame radiuses and time instants. The maximum absolute error percentage in the turbulent flame radius was found to be 5.46%, 4.98%, and 3.46% for diesel, GTL, and the 50/50 blend, respectively.
- In addition, it was observed that there is a good agreement between model 2 and the CFD simulations outputs, where the maximum absolute error percentage was found to be 6.58% (at $u' = 1.5\text{m/s}$) and 2.57% (at $u' = 2.5\text{m/s}$) for GTL and the 50/50 blend, respectively.
- The developed ML models offer ready-to-use models that can be combined with, for instance, CFD software for studies on turbulent combustion, in addition to being useful for assessing the findings of experiments or kinetic modeling.

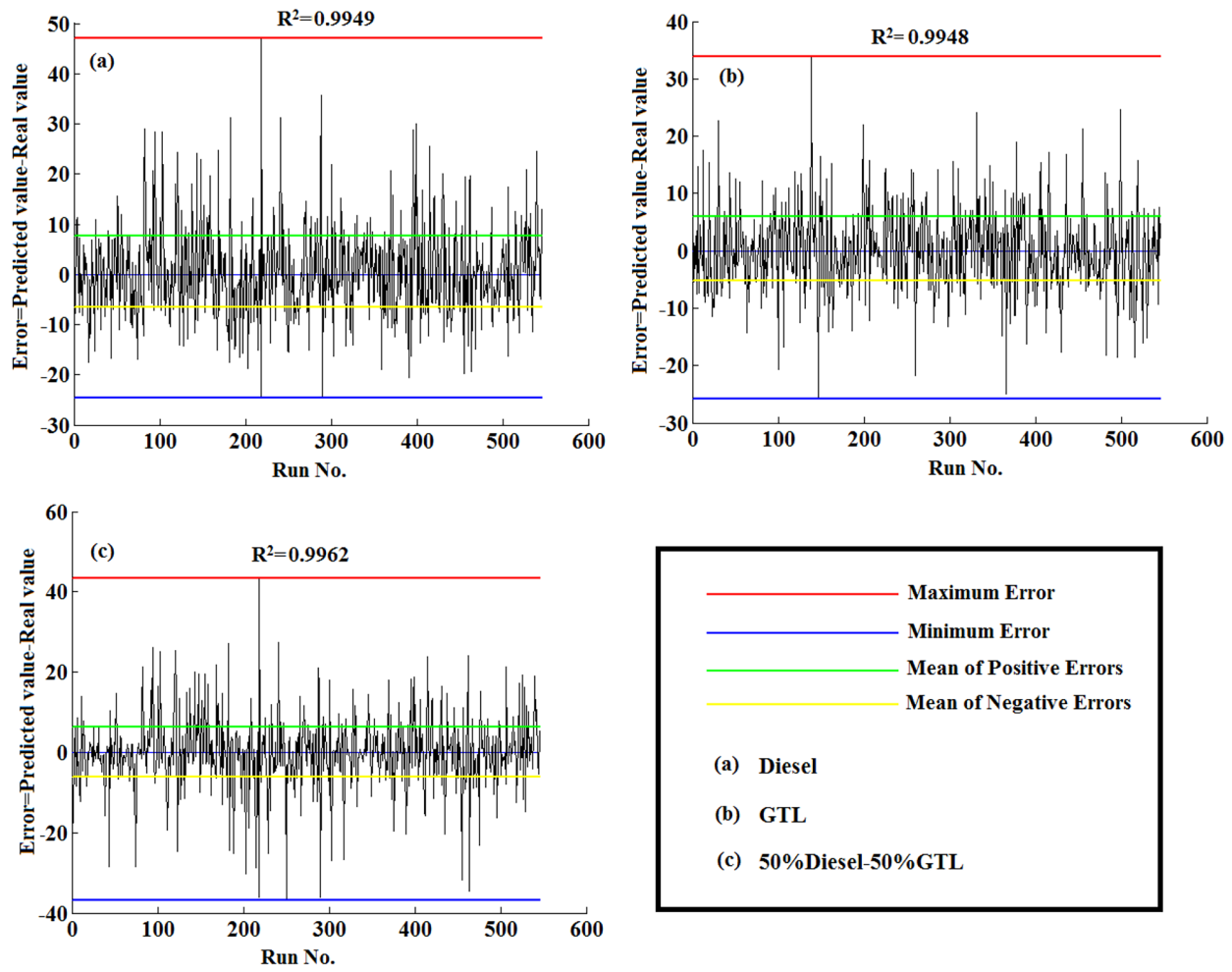


Fig. 9 Error values of AI-predicted flame speed for three different fuels

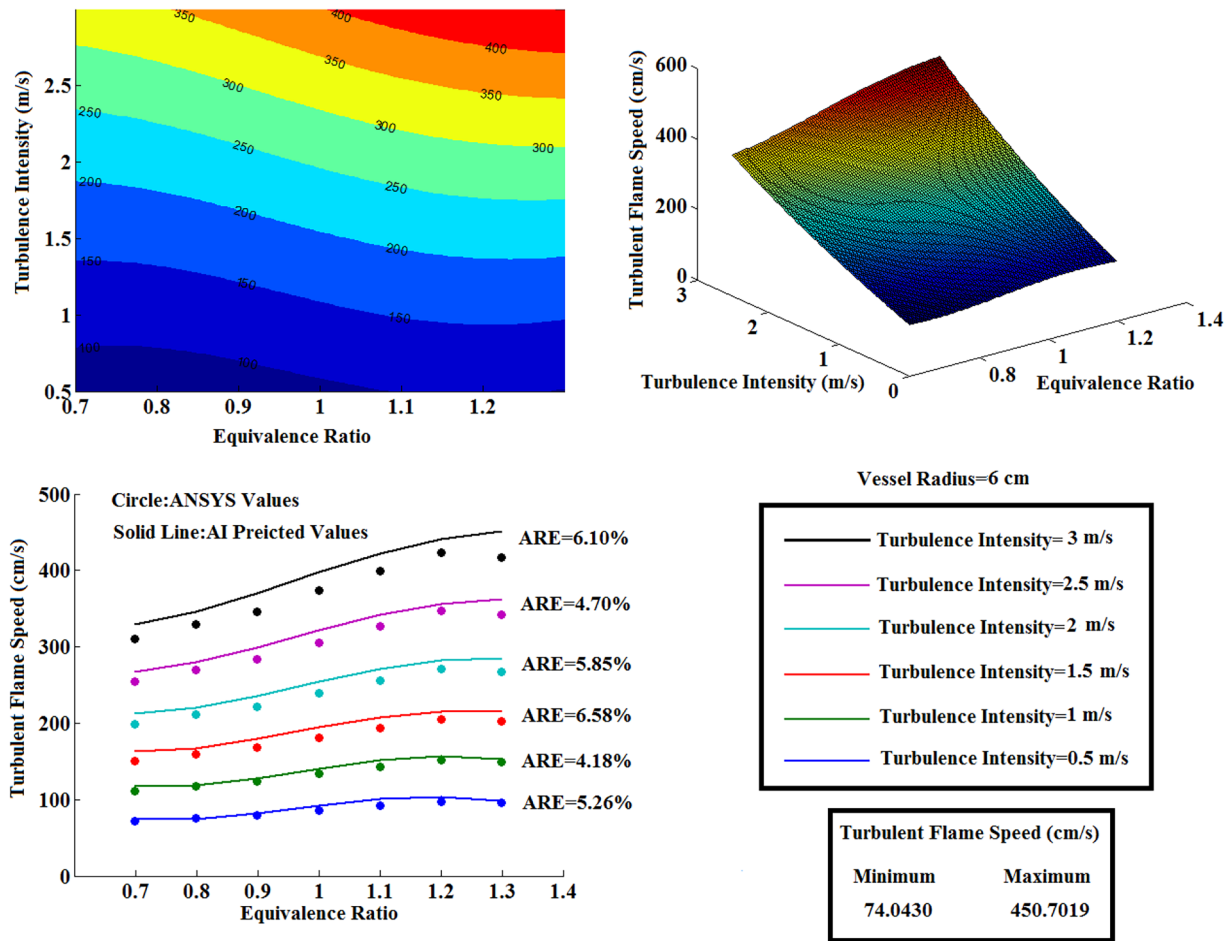


Fig. 10 3D plot and contour plot of AI-predicted and 2D plot of CFD and AI-predicted flame speed for GTL as a function of equivalence ratio and turbulent intensity

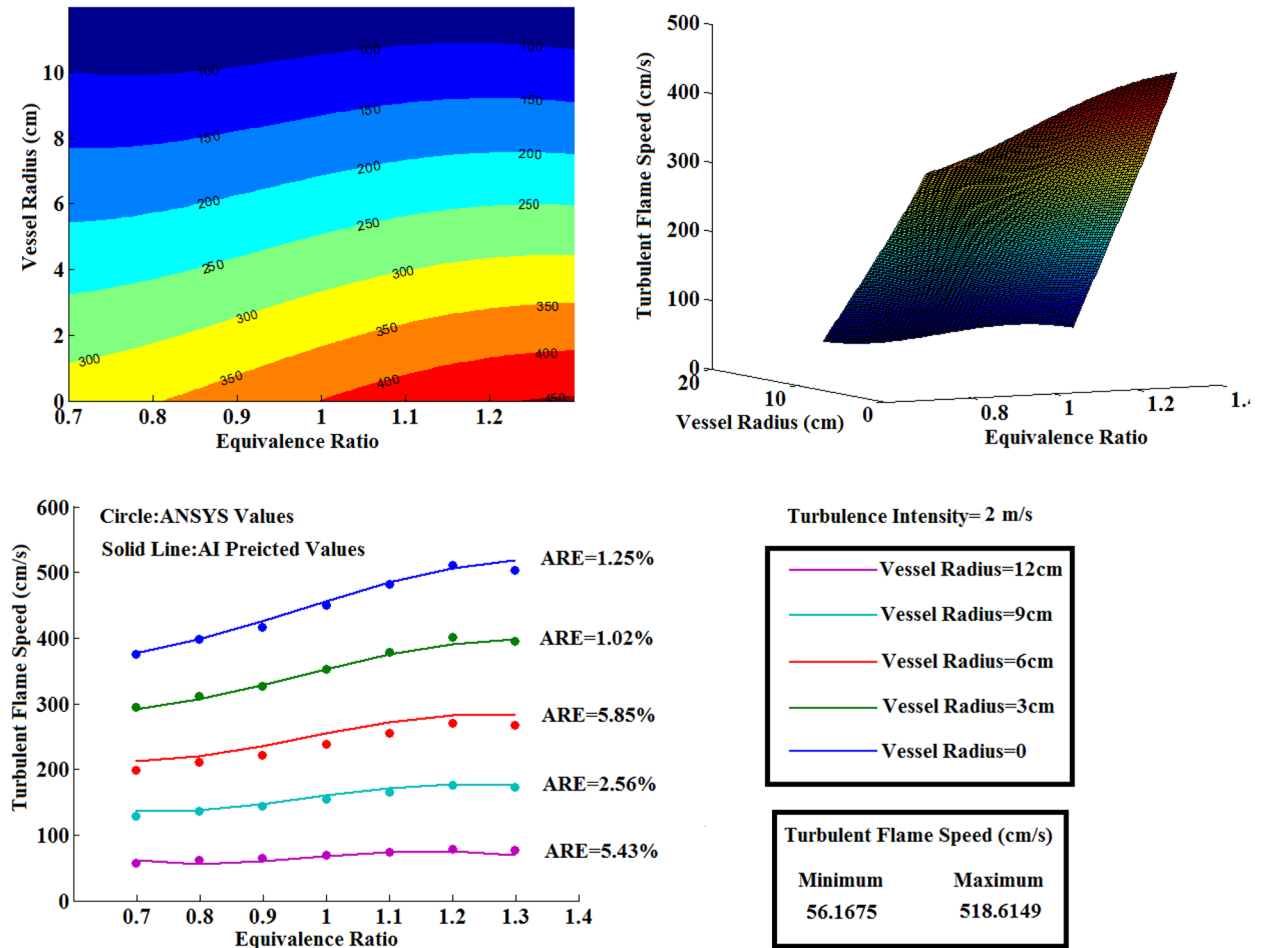


Fig. 11 3D plot and contour plot of AI-predicted and 2D plot of CFD and AI-predicted flame speed for GTL as a function of equivalence ratio and vessel radius

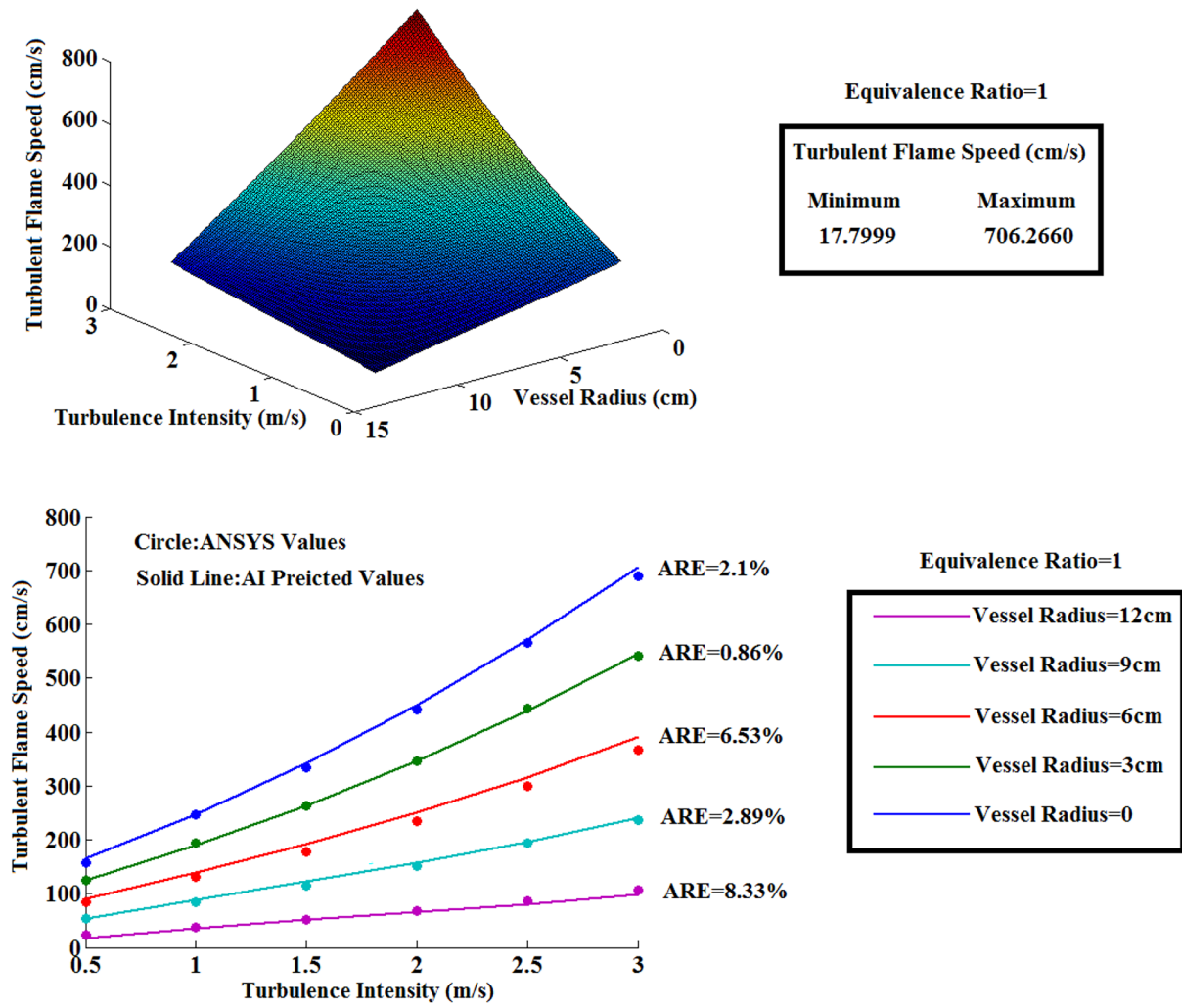


Fig. 12 3D plot of AI-predicted and 2D plot of CFD and AI-predicted flame speed for Diesel as a function of turbulence intensity and vessel radius

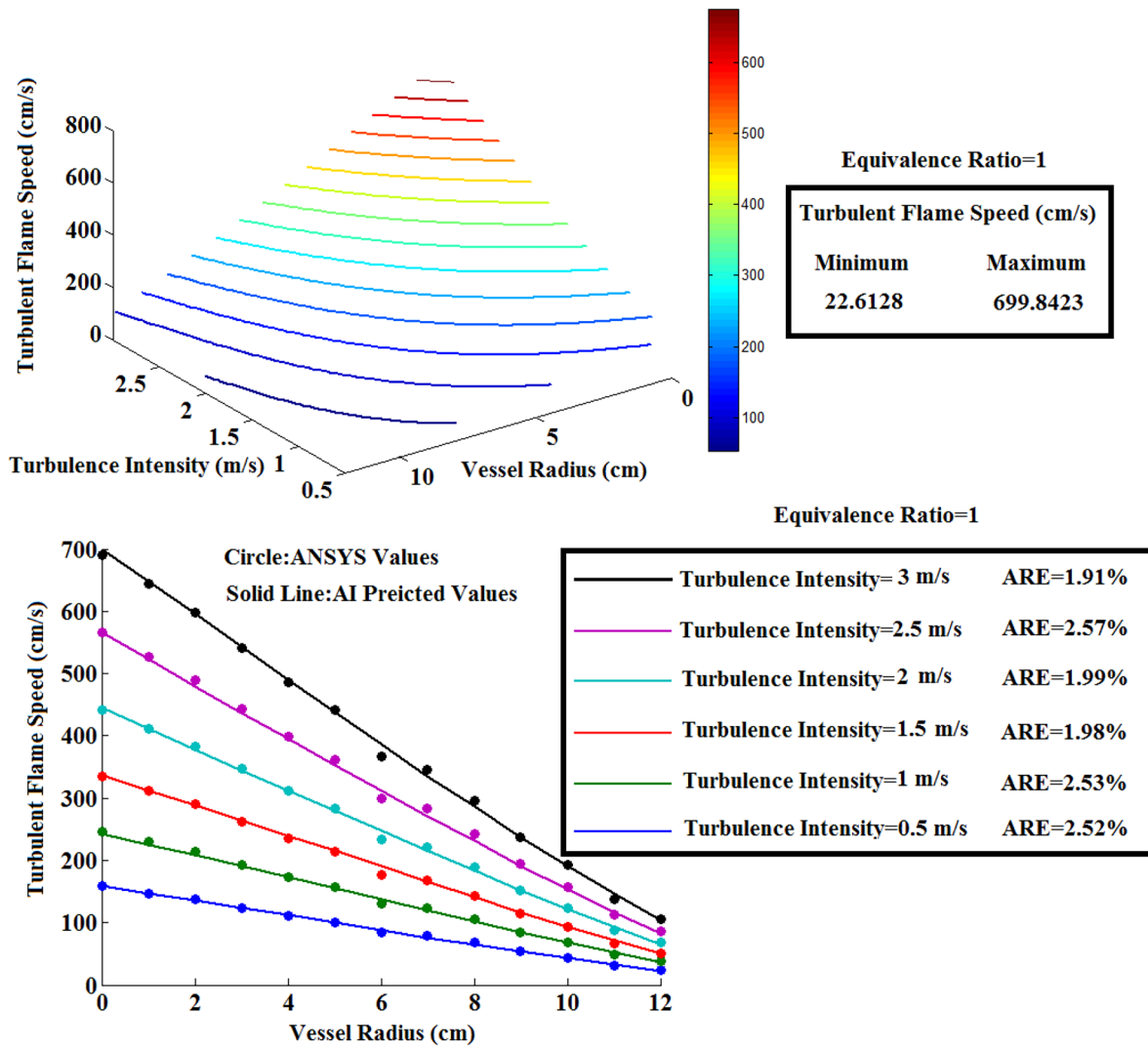


Fig. 13 Contour plot of AI-predicted and 2D plot of CFD and AI-predicted flame speed for blend fuel as a function of turbulence intensity and vessel radius

Table 2 Minimum and maximum values of response for different fuels

Fuel	Model 1			Model 2			
	Response	Operating parameters		Response	Operating parameters		
	Flame radius (cm)	Equivalence ratio, ϕ	Time (ms)	Flame speed (cm/s)	Equivalence ratio	Turbulence intensity, u' (m/s)	Vessel radius, r (cm)
Diesel							
Min	0.47206	0.7	5	13.2948	0.84585	0.5177	12
Max	6.9298	1.1156	30	831.0796	1.2996	3	0.0027006
GTL							
Min	0.64792	0.7003	5	12.4148	1.3	0.5	12
Max	7.5088	1.1049	30	797.6698	1.2923	3	0.017375
Blend							
Min	0.59122	0.7	5	20.0713	0.70592	0.5	12
Max	7.4517	1.1204	30	810.564	1.3	3	0.026625

Acknowledgement Open Access Funding Provided by the Qatar National Library.

Funding Open Access funding provided by the Qatar National Library.

Data Availability The data supporting the findings of this study are available in the repository named "Premixed Turbulent Combustion of Diesel, GTL, 50% to 50% Blend- Zimont TFC Model" at the following direct <https://doi.org/10.17632/ts2jd8zc9r.3>.

Open Access This article is licensed under a Creative Commons Attribution 4.0 International License, which permits use, sharing, adaptation, distribution and reproduction in any medium or format, as long as you give appropriate credit to the original author(s) and the source, provide a link to the Creative Commons licence, and indicate if changes were made. The images or other third party material in this article are included in the article's Creative Commons licence, unless indicated otherwise in a credit line to the material. If material is not included in the article's Creative Commons licence and your intended use is not permitted by statutory regulation or exceeds the permitted use, you will need to obtain permission directly from the copyright holder. To view a copy of this licence, visit <http://creativecommons.org/licenses/by/4.0/>.

References

1. P. Palies, The flame displacement speed: a key quantity for turbulent combustion and combustion instability. *Int. J. Spray Combust. Dyn.* **14**(1–2), 4–16 (2022). <https://doi.org/10.1177/17568277221081298>
2. J.F. Driscoll, J.H. Chen, A.W. Skiba, C.D. Carter, E.R. Hawkes, H. Wang, Premixed flames subjected to extreme turbulence: Some questions and recent answers. *Prog. Energy Combust. Sci.* **76**, 100802 (2020). <https://doi.org/10.1016/j.pecs.2019.100802>
3. K. Bray, M. Champion, P.A. Libby, N. Swaminathan, Scalar dissipation and mean reaction rates in premixed turbulent combustion. *Combust. Flame* **158**(10), 2017–2022 (2011). <https://doi.org/10.1016/j.combustflame.2011.03.009>
4. G. Fru, D. Thévenin, G. Janiga, Impact of turbulence intensity and equivalence ratio on the burning rate of premixed methane-air flames. *Energies (Basel)* **4**(6), 878–893 (2011). <https://doi.org/10.3390/en4060878>
5. T. Turek, *Combustion Analysis for Flame Stability Predictions at Ground Level and Altitude in Aviation Gas Turbine Engines with Low Emissions Combustors* (University of Toronto, 2015)
6. A. Morones et al., Laminar and turbulent flame speeds for natural gas/hydrogen blends. In: *Proceedings of the ASME Turbo Expo*, 2014, vol. 4B, no. June. <https://doi.org/10.1115/GT2014-26742>.
7. M. Farokhi, M. Birouk, Modeling of the gas-phase combustion of a grate-firing biomass furnace using an extended approach of Eddy Dissipation Concept. *Fuel* **227**(May), 412–423 (2018). <https://doi.org/10.1016/j.fuel.2018.04.102>
8. Sadeq et al., Combustion and emissions of a diesel engine utilizing novel intake manifold designs and running on alternative fuels. *Fuel* **16**(2361), 1–19 (2019)
9. J. Delbeke, A. Runge-Metzger, Y. Slingenberg, and J. Werksman, *The paris agreement*. 2019, pp. 24–45. doi: <https://doi.org/10.4324/9789276082569-2>.
10. S. Samim, A.M. Sadeq, S.F. Ahmed, Measurements of laminar flame speeds of gas-to-liquid-diesel fuel blends. *J. Energy Resour. Technol. Trans. ASME* **138**(5), 1–8 (2016). <https://doi.org/10.1115/1.4033627>
11. Shell Qatar, "Shell Qatar, 2010, 'Pearl GTL, Overview'. 2010. <https://www.shell.com/about-us/major-projects/pearl-gtl/pearl-gtl-an-overview.html>. Accessed 23 Aug 2022.
12. A.M. Sadiq, A.K. Sleiti, S.F. Ahmed, Turbulent flames in enclosed combustion chambers: characteristics and visualization—a review. *J. Energy Resour. Technol.* (2020). <https://doi.org/10.1115/1.4046460>
13. A.M. Sadeq, S.F. Ahmed, A.K. Sleiti, Transient 3D simulations of turbulent premixed flames of gas-to-liquid (GTL) fuel in a fan-stirred combustion vessel. *Fuel* **291**(February), 120184 (2021). <https://doi.org/10.1016/j.fuel.2021.120184>
14. H.J. Curran, Developing detailed chemical kinetic mechanisms for fuel combustion. *Proc. Combust. Inst.* **37**(1), 57–81 (2019). <https://doi.org/10.1016/J.PROCI.2018.06.054>
15. C.K. Westbrook, H.J. Curran, Detailed kinetics of fossil and renewable fuel combustion. *Comput. Aided Chem. Eng.* **45**, 363–443 (2019). <https://doi.org/10.1016/B978-0-444-64087-1.00007-3>
16. K.P. Shrestha et al., A detailed chemical insights into the kinetics of diethyl ether enhancing ammonia combustion and the importance of NOx recycling mechanism. *Fuel Communications* **10**, 100051 (2022). <https://doi.org/10.1016/J.JFUECO.2022.100051>
17. J.H. Chen, Petascale direct numerical simulation of turbulent combustion—fundamental insights towards predictive models. *Proc. Combust. Inst.* **33**(1), 99–123 (2011). <https://doi.org/10.1016/J.PROCI.2010.09.012>
18. T. Lu, C.K. Law, Toward accommodating realistic fuel chemistry in large-scale computations. *Prog. Energy Combust. Sci.* **35**(2), 192–215 (2009). <https://doi.org/10.1016/J.PECS.2008.10.002>
19. Z.M. Nikolaou, N. Swaminathan, J.Y. Chen, Evaluation of a reduced mechanism for turbulent premixed combustion. *Combust. Flame* **161**(12), 3085–3099 (2014). <https://doi.org/10.1016/J.COMBUSTFLAME.2014.06.013>
20. R. Amirante, E. Distaso, P. Tamburrano, R.D. Reitz, Analytical correlations for modeling the laminar flame speed of natural gas surrogate mixtures. *Energy Proc.* **126**, 850–857 (2017). <https://doi.org/10.1016/J.EGYPRO.2017.08.289>
21. J. Wallesten, A. Lipatnikov, J. Chomiak, Modeling of stratified combustion in a direct-ignition, spark-ignition engine accounting for complex chemistry. *Proc. Combust. Inst.* **29**(1), 703–709 (2002). [https://doi.org/10.1016/S1540-7489\(02\)80090-6](https://doi.org/10.1016/S1540-7489(02)80090-6)
22. A.A. Konnov, A. Mohammad, V.R. Kishore, N. il Kim, C. Prathap, S. Kumar, A comprehensive review of measurements and data analysis of laminar burning velocities for various fuel+air mixtures. *Prog. Energy Combust. Sci.* **68**, 197–267 (2018). <https://doi.org/10.1016/J.PECS.2018.05.003>
23. S.Y. Liao, D.M. Jiang, Q. Cheng, Determination of laminar burning velocities for natural gas. *Fuel* **83**(9), 1247–1250 (2004). <https://doi.org/10.1016/J.FUEL.2003.12.001>
24. U.C. Müller, M. Bollig, N. Peters, Approximations for burning velocities and markstein numbers for lean hydrocarbon and methanol flames. *Combust. Flame* **108**(3), 349–356 (1997). [https://doi.org/10.1016/S0010-2180\(96\)00110-1](https://doi.org/10.1016/S0010-2180(96)00110-1)
25. E. Hu et al., Laminar flame speeds and ignition delay times of methane–air mixtures at elevated temperatures and pressures. *Fuel* **158**, 1–10 (2015). <https://doi.org/10.1016/J.FUEL.2015.05.010>
26. F.H.V. Coppens, J. de Ruyck, A.A. Konnov, The effects of composition on burning velocity and nitric oxide formation in laminar premixed flames of CH₄ + H₂ + O₂ + N₂. *Combust. Flame* **149**(4), 409–417 (2007). <https://doi.org/10.1016/J.COMBUSTFLAME.2007.02.004>
27. F. vom Lehn, B. Brosius, R. Broda, L. Cai, H. Pitsch, Using machine learning with target-specific feature sets for structure-property relationship modeling of octane numbers and octane

- sensitivity. *Fuel* **281**, 118772 (2020). <https://doi.org/10.1016/J.FUEL.2020.118772>
28. T. Kessler, P.C. John, J. Zhu, C.S. McEnally, L.D. Pfefferle, J.H. Mack, A comparison of computational models for predicting yield sooting index. *Proc. Combust. Inst.* **38**(1), 1385–1393 (2021). <https://doi.org/10.1016/J.PROCI.2020.07.009>
 29. P.P. Popov et al., Machine learning-assisted early ignition prediction in a complex flow. *Combust. Flame* **206**, 451–466 (2019). <https://doi.org/10.1016/J.COMBUSTFLAME.2019.05.014>
 30. K. Wan, C. Barnaud, L. Vervisch, P. Domingo, Chemistry reduction using machine learning trained from non-premixed micro-mixing modeling: Application to DNS of a syngas turbulent oxy-flame with side-wall effects. *Combust. Flame* **220**, 119–129 (2020). <https://doi.org/10.1016/J.COMBUSTFLAME.2020.06.008>
 31. A.H. Moghaddam, J. Sargolzaei, M.H. Asl, F. Derakhshanfard, Effect of different parameters on WEPS production and thermal behavior prediction using artificial neural network (ANN). *Polym. Plast. Technol. Eng.* **51**(5), 480–486 (2012). <https://doi.org/10.1080/03602559.2011.651243>
 32. F. Mahmoudian, A.H. Moghaddam, S.M. Davachi, Genetic-based multi-objective optimization of alkylation process by a hybrid model of statistical and artificial intelligence approaches. *Can. J. Chem. Eng.* **100**(1), 90–102 (2022). <https://doi.org/10.1002/cjce.24072>
 33. A.H. Moghaddam, J. Shayegan, J. Sargolzaei, Investigating and modeling the cleaning-in-place process for retrieving the membrane permeate flux: Case study of hydrophilic polyethersulfone (PES). *J. Taiwan Inst. Chem. Eng.* **62**, 150–157 (2016). <https://doi.org/10.1016/j.jtice.2016.01.024>
 34. S. Rashidi, A.H. Moghaddam, Investigation and optimization of anaerobic system for treatment of seafood processing wastewater. *Chem. Pap.* **75**(9), 4649–4660 (2021). <https://doi.org/10.1007/s11696-021-01675-y>
 35. K. Malik, M. Zbikowski, A. Teodorczyk, Laminar burning velocity model based on deep neural network for hydrogen and propane with air. *Energies (Basel)* (2020). <https://doi.org/10.3390/en13133381>
 36. R.K. Mehra, H. Duan, S. Luo, F. Ma, Laminar burning velocity of hydrogen and carbon-monoxide enriched natural gas (HyCONG): an experimental and artificial neural network study. *Fuel* **246**, 476–490 (2019). <https://doi.org/10.1016/j.fuel.2019.03.003>
 37. S. Eckart, R. Prieler, C. Hochenauer, H. Krause, Application and comparison of multiple machine learning techniques for the calculation of laminar burning velocity for hydrogen-methane mixtures. *Therm Sci Eng Progress* (2022). <https://doi.org/10.1016/j.tsep.2022.101306>
 38. F. vom Lehn, L. Cai, B. Copa Cáceres, H. Pitsch, Exploring the fuel structure dependence of laminar burning velocity: a machine learning based group contribution approach. *Combust. Flame* (2021). <https://doi.org/10.1016/j.combustflame.2021.111525>
 39. Z. Wan, Q.-D. Wang, B.-Y. Wang, J. Liang, Development of machine learning models for the prediction of laminar flame speeds of hydrocarbon and oxygenated fuels. *Fuel Commun.* **12**, 100071 (2022). <https://doi.org/10.1016/j.jfueco.2022.100071>
 40. A.M. Sadeq, S.F. Ahmed, A.K. Sleiti, Dataset for transient 3D simulations of turbulent premixed flames of Gas-to-Liquid (GTL) fuel. *Data Brief* (2021). <https://doi.org/10.1016/j.dib.2021.106956>
 41. A.M. Sadeq, S.F. Ahmed, A.K. Sleiti, Premixed turbulent combustion of diesel, GTL, 50% to 50% Blend-Zimont TFC model. *Mendeley Data* (2021). <https://doi.org/10.17632/ts2jd8zc9r.3>

Publisher's Note Springer Nature remains neutral with regard to jurisdictional claims in published maps and institutional affiliations.